Published in final edited form as:
Brain Res. 2011 January 7; 1367: 50–61. doi:10.1016/j.brainres.2010.10.056.

Immunocytochemical distribution of WARP (von Willebrand A domain-related protein) in the inner ear

Trac Duong[1], **Ivan A. Lopez**[1], **Akira Ishiyama**[1], and **Gail Ishiyama**[§,2]

[1]Surgery Department, Division of Head and Neck, "David Geffen" School of Medicine, at UCLA, Los Angeles California, USA

[2]Neurology Department, "David Geffen" School of Medicine, at UCLA, Los Angeles California, USA

Abstract

The basic components of the epithelial, perineural and perivascular basement membranes in the inner ear have been well-documented in several animal models and in the human inner ear. The von Willebrand A domain-related protein (WARP) is an extracellular matrix molecule with restricted expression in cartilage, and a subset of basement membranes in peripheral nerves, muscle and central nervous system vasculature. It has been suggested that WARP have an important role in maintaining the blood-brain barrier. To date no studies on WARP distribution have been performed in the inner that is equipped with an intricate vasculature network. In the present study we determined the distribution of WARP by immunocytochemistry in the human inner ear using auditory and vestibular endorgans microdissected from human temporal bones obtained at autopsy. All subjects (n=5, ages 55-87 years old) had documented normal auditory and vestibular function. We also determined the WARP immunolocalization in the mouse inner ear. WARP-immunoreactivity localized to the vasculature throughout the stroma of the cristae ampullaris, the maculae utricle and saccule in the human and mouse. In the human and mouse inner ear, WARP-immunoreactivity delineated blood vessels located in the stria vascularis, spiral ligament, sub-basilar region, stromal tissue, and the spiral and vestibular ganglia. The distinct localization of WARP in the inner ear vasculature suggests an important role in maintaining its integrity. In addition, WARP allows delineation of microvessels in the inner ear allowing the study of vascular pathology in the development of otological diseases.

Keywords

VWA-1; basement membrane; blood vessels; cochlea; extracellular matrix; inner ear microvasculature

1. Introduction

The composition of the human inner ear basement membranes (BMs) was recently investigated in the cochlea and vestibule from subjects with normal audiovestibular function

[§]Corresponding author: Gail Ishiyama M.D., Reed Neurological Research Center, David Geffen UCLA School of Medicine, Department of Neurology, 710 Westwood Blvd. Box 957619, Los Angeles, CA 90095. Phone; 310-825-5331, gishiyama@mednet.ucla.edu.

(Ishiyama et al., 2009). Collagen IVα2, laminin-β2, and nidogen-1 colocalized within the human cochlear and vestibular BMs, as well as perivascular and perineural BMs in zones which demarcate endolymph from perilymph, suggestive of BM involvement in the regulation of water and ionic homeostasis in the mammalian inner ear. The distribution of these extracellular matrix (ECM) proteins in the human inner ear was similar to rodent models, where available data exists for comparison, demonstrating conservation of BM composition, and confirming the use of these animal models for inner ear BM pathologies.

In addition to performing structural roles, ECM proteins have diverse functions which include mediating collagen fibrillar architecture, bridging between macromolecular networks, binding growth factors and influencing cell differentiation, migration or adhesion, and providing linkages between cells and the ECM (Heinegard et al., 2002). Many of these matrix proteins are modular in structure, composed of protein domains (Allen et al., 2008; 2009). The identification of BM and ECM proteins in the inner ear may be clinically relevant given the identification of DFNA9 deafness and association with mutations in the secreted ECM protein cochlin (Robertson et al., 2006). One of the domains which is found in a multitude of ECM proteins is the A domain, first described in von Willebrand factor (VWA domain) (Fitzgerald et al., 2002).

A new member of the von Willebrand factor A domain superfamily was recently described: WARP (von Willebrand factor A domain-related protein), encoded by the Vwa1 gene, that may have evolved from a collagen-like molecule (Fitzgerald et al., 2002). The WARP protein comprises a single N-terminal VWA domain containing a putative metal ion-dependent adhesion site motif, two fibronectin type III repeats, and a unique C-terminal segment. WARP is a multimeric component of the chondrocyte pericellular matrix in articular cartilage and intervertebral disc, where it interacts with the BM heparan sulfate proteoglycan perlecan (Allen et al., 2006). WARP is expressed in the vasculature of neural tissues, in the BMs of the peripheral nervous system, and in the apical ectodermal ridge of developing limb buds, and in skeletal and cardiac muscle (Allen et al., 2008, 2009). Among the suggested functions of WARP is its role in maintaining the blood-brain barrier (Allen et al., 2008). The inner ear is equipped with an intricate vasculature network (Axelsson, 1968; Bachor et al., 2001; Hawkins, 1976; Lawrence, 1980; Miller, 1995; Nakashima, 2003; Shi, 2009), as well as perivascular and perineural basement membrane proteins (Ishiyama et al., 2009). Thus in the present study we investigate the immunolocalization of WARP in the human and mouse inner ear.

2. Results

2.1 WARP-immunoreactivity (WARP-IR) distribution in the human inner ear

WARP-IR in the cochlea—WARP-IR localized within the vasculature of the cochlea in human. Figure 1A shows a midmodiolar (cross) section of the cochlea, WARP-IR was visualized by indirect immunohistochemistry using horseradish peroxidase and the chromogen diaminobenzidine. WARP-IR was localized in blood vessels at all levels from the base to apical portion. Figure 1B shows WARP-immunofluorescence in the organ of Corti (mid-apical portion). WARP immunofluorescence (red color) delineated the vasculature in the stria vascularis, spiral ligament and blood vessels underneath the basilar lamina. Figure 1C is a low magnification view of the hook region of the cochlea. Figure C1 and C2 shows WARP-IR in the stria vascularis blood vessels and Rosenthal's canal respectively. Figure 1D, 1D1, 1D2, and 1D3 shows WARP-IR in blood vessels of the spiral ganglia at the apical, middle, basal and hook region respectively. There was no discernible regional variation of WARP-IR in the vasculature from the apical to the basal portion of the cochlea.

Colocalization of WARP and smooth muscle actin (SMA) in the stria vascularis and lateral wall

Stria vascularis: Figure 2A1 shows WARP-IR in blood vessels in the stria vascularis (red color). Figure 2A1 shows the same section stained with antibodies against SMA (green color). Figure 2A2 is a merged image from A and A1. WARP and SMA colocalized in some blood vessels (yellow color), and other blood vessels stained with either WARP or SMA only.

WARP-IR distribution in the human cochlear lateral wall (surface preparation) showing immunolocalization of WARP-IR (red) and SMA (green) in the lateral wall. Figure 2B and 2B1 shows WARP-IR and SMA respectively in blood vessels of the lateral wall. As in the stria vascularis some blood vessels were immunoreactive only to WARP (Fig 2B2) or SMA. (Fig 2B2 is the merged image from 2B and 2B1). Figure 2B3 shows a high magnification view that WARP and SMA colocalized in some blood vessels. Figure 2C corroborates WARP immunofluorescence with the use of indirect immunohistochemistry (HRP-DAB). WARP-IR delineated clearly the blood vessels of the lateral wall. Figure 2C1 is a high magnification view from Figure 2C. Figure 2D shows a thin section of the spiral ligament. The blood vessels are well-delineated by WARP-IR.

WARP-IR in vestibular endorgans—In the three cristae ampullaris (horizontal, posterior and superior), WARP-IR was localized in blood vessels located in the cristae stroma. Figure 3A and 3A1 shows WARP-IR in the central and peripheral portion of the horizontal crista. WARP-IR was present in blood vessels from the planum semilunatum to the central region of the cristae (Fig 3A and 3A1). A similar pattern was seen in the posterior and superior cristae. The hair cells and supporting cells in the vestibular sensory epithelia showed no WARP-IR (Fig 3A1). In a similar fashion, WARP-IR was present in the vasculature of the maculae utricle (Fig 3B). Indirect immunoreactivity using HRP-DAB shows a similar pattern in the saccule (Fig 3C). Higher magnification view in the insert to the left shows that WARP is confined to blood vessels of the stroma. WARP-IR was also present in the vasculature of the vestibular (Scarpa's) ganglia (Fig 3D and 1D1). Figure 3D shows colocalization of WARP (red color) and calretinin a marker for vestibular ganglia neurons (green color). Both proteins are located in different compartments. Indirect immunostaining shows that WARP is confined to blood vessels; vestibular ganglion neurons were non-immunoreactive (Fig 3D1).

2.2 WARP-IR distribution in the mouse inner ear

WARP-IR distribution in the cochlea—WARP-IR was present in the vasculature of the spiral ligament, spiral prominence and the stria vascularis in the mouse (Fig 4A). Colocalization of WARP and SMA in blood vessels of the stria vascularis is shown in Figure 4A1. WARP-IR was not observed in inner and outer hair cells, supporting cells. As in the human cochlea, there was no discernible regional variation of WARP-IR pattern from the basal to the apical portion of the mice cochlea. Figure 4B and 4B1 shows WARP-IR and SMA in blood vessels of the spiral ganglia at basal and mid apical portion respectively. WARP colocalizes with SMA was confined to blood vessels and arteries (Fig 4B). Spiral ganglia neurons were not immunoreactive to WARP. WARP-IR was also evident in midmodiolar arteries of the cochlea. Figure 4C shows colocalization of WARP (red color) and SMA (green color) in midmodiolar arteries. WARP delineates the artery and SMA is located mainly at the peripheral portion (Fig 4C).

WARP-IR in vestibular endorgans—In the mouse macula utricle and sacule, WARP-IR was seen also in BMs of the blood vessels located at the stroma (Fig 5A and 5B respectively). Colocalization of WARP with SMA colocalized in blood vessels of the utricle

(Fig 5A1) and saccule (Fig 5B1) stroma. In the three cristae ampullares (horizontal, posterior and superior), WARP-IR was seen in the blood vessels running throughout the crista stroma. Figure 5C shows WARP and SMA colocalization in blood vessels of the stroma. As with the human cristae this pattern of WARP-IR was seen from the central region to the peripheral (planum semilunatum) region. WARP-IR was not present in the sensory epithelia. In the mice vestibular (Scarpa's) ganglia, Figure 5D shows that WARP-IR colocalized with SMA to the blood vessels. Vestibular ganglia neurons were not immunoreactive (Fig 5D).

WARP-IR controls

Positive controls for the WARP: Central nervous tissue (brainstem) from the same patients (Fig 6A), as well as mice cerebellar cortex (Fig 6B and 6B1). Figure 6A shows WARP-IR in perivascular BMs of the brainstem (pons). Note that small and large size blood vessels were stained with WARP antibodies. Figure 6B shows WARP immunofluorescence in blood vessels of the mice cerebellar cortex. Figure 6B1 shows WARP-IR in another mice cerebellum section using HRR-DAB that corroborated WARP immunostaining. WARP-IR in the vasculature of the nervous tissue was similar to that identified by X-gal staining of the Vwa1+/βgal mouse (Allen et al., 2008). Negative controls (incubation with normal serum or no primary antibody) did not demonstrate immunoreactivity within the vestibular or cochlear tissues. Figure 6C demonstrates the cross-section of the human utricle immunostained with all the reagents except for the WARP antibody, no specific immunoreactivity was observed. The specificity of the WARP antibody was investigated using protein extracts from the mice inner ear and human cerebellum. A single band of approximately 55 kDa was observed (Fig 7).

3. Discussion

WARP-IR was detected in the human and mice inner ear vasculature. Blood vessels are highly organized and complex structures, which autonomously regulate the blood flow, to provide an optimal level of oxygen and nutrients. The ECM in blood vessel contributes substantially to the diverse functions of the vasculature (Eble and Noland, 2009). The ECM constitutes the scaffold which provides the structure of the vessel wall which by vasoconstriction, the blood flow and pressure is regulated. In prior studies, WARP-expressing cells were found in the vasa nervorum, and the BMs of the microvasculature within peripheral nerves (Allen et al., 2008). Notably, WARP is not present in all vasculature, as it is absent from the sinusoidal capillaries in the liver (Allen et al., 2008). To date, there are no descriptions of the localization of WARP in the inner ear.

The ubiquitous distribution throughout the vasculature of the inner ear suggests that WARP may have a structural or maintenance role of the capillaries and arteries of the cochlea and vestibule. Allen et al. (2008) have suggested that WARP may have an important role in maintaining the blood-brain barrier throughout life. There are only a handful of studies of WARP expression in mice, initially discovered in mouse chondrocytes (Fitzgerald et al., 2002; Allen et al., 2006, 2008, 2009). Further studies on WARP expression showed that WARP is present in the vasculature of neural tissues and in basement membrane structures and cardiac muscle (Allen et al., 2008). A recent study shows that WARP-null mice are healthy, viable and no overt abnormalities (Allen et al., 2009). However, the null mice demonstrated diminished pain sensitivity and motor abnormalities. WARP is hypothesized to play an important role in stabilizing the association of collagenous interstitial matrix at the Schwann cells basement membrane. Previous studies in human and mice inner ear have show an abundance of collagen, nidogen, laminin and several other basement membranes located in the perineurium and the vasculature (Ishiyama et al., 2009). Whether or not

alterations in WARP expression in the inner ear results in auditory or vestibular deficits remains to be determined.

There are several diseases in which WARP expression maybe altered, whether or not WARP maybe involved it remains to be determined. An inner ear disease in which vasculature is affected is Norrie disease (Rehm et al., 2002). Norrin, the protein product of the Norrie disease gene, is a secreted protein of unknown biochemical function (Xu et al., 2004). The characteristic feature of Norrie disease is congenial bilateral blindness, with a partial avascularity of the retina. Most patients also manifest hearing loss (Rehm et al., 2002). Of note, the mouse model of Norrie disease shows abnormal vasculature in the stria vascularis.

We used young mice to study WARP distribution and found a similar localization in the vasculature of the cochlea and vestibule. Studies during pre- and postnatal period and aging would help to determine the time course of expression of WARP in the inner ear. mRNA studies would also help to corroborate WARP expression in the inner ear. WARP may be also expressed in perineural or epithelial basement membranes of the inner ear and this expression may be developmentally determined. The differences in WARP immunolocalization in previous studies in other systems may be secondary to the type of antibodies. Allen et al. (2008) uses a sheep antibody raised against full length recombinant WARP purified from the media of transfected 293-EBNA cells. In that study, WARP was located in the mice vasculature nervous system and in perineural basement membranes, and developing muscle tissue and articular cartilage (Allen 2009). In another study Allen et al. used a rabbit polyclonal antisera against VWA domain and C-terminal domains of WARP, using the GST-VWA domain (amino acids 21-212) and the maltose-binding protein-C-terminal domain (amino acids 389-415) fusion proteins, expressed in bacteria as antigens. These antibodies stain the developing articular cartilage (Allen et al 2006). In the present study, we used a commercial rabbit polyclonal affinity purified antibodies raised against von Willebrand factor A domain containing 1 recombinant epitope signature tag. We detected a band of approximately 50-55 kDa using WARP rabbit polyclonal antibodies and western blot extracts from the mice cochlea and human cerebellum. Fitzgerald et al. (2002) reported a 45kDA protein in extract from WARP transfected cells. The difference in the antibody source as well as the pretreatment likely account for the difference of the bands detected in our study. Also, it is possible that more than one isoform of WARP may be present in the inner ear.

Given the complex interaction of WARP with several proteins located in perivascular BMs, an altered expression of WARP in the inner ear may have pathophysiological significance. The inner ear microvasculature plays an essential role in establishing homeostasis (Miller et al., 1995). Disturbances in the microvasculature of the cochlea and vestibular labyrinth are suspected to contribute to otologic disorders such as Meniere's disease, sudden deafness, congenital hearing loss and presbycusis (Hawkins, 1973, McCall et al., 2009). The stria vascularis is a rich vascular plexus in the cochlea with ability to regulate electrolytes (Axelsson, 1968; Duball et al., 1980), and is also believed to be the one of the primary sites of endolymph production. Atrophy of the stria vascularis in patients with Meniere's disease compared to normal controls has been documented (Masutani et al., 1992; Ishiyama et al., 2007), as well as in aging, ototoxicity and noise exposure (Hawkins, 1973). A thickening of the strial capillary BMs in the animal model of Alport's syndrome, the COL4A3 deficient mouse, is associated with hearing loss (Cosgrove et al., 1998). Recent studies using MRI, laser Doppler flowmetry and ultrasonography suggest that disordered cochlear blood flow may contribute to noise-induced hearing loss, endolymphatic hydrops and presbycusis (Nakashima et al., 2003). WARP-IR in the stria vascularis and spiral ligament provides excellent visualization of the interior wall of blood vessels of differential diameters to evaluate the microvasculature in otopathologies.

The anatomy of inner ear microvessels has been studied using various techniques such as chemical staining with benzidine, vessel injection and electron microscopy (Axelsson, 1968; Mazzoni, 1990; Hawkins, 1976; Lawrence, 1980; Miller et al., 1995; Bachor et al., 2001). In the present study, WARP proves to be an effective and sensitive marker to delineate blood vessel vasculature in the mouse and human inner ear, adding sensitivity by colocalization with SMA-IR. Other markers, such as desmin, trpomyosin, neurogenin-2 (NG2), Trh-1 and isolectin, have been applied to study the inner ear vasculature (Shi et al., 2008; Shi, 2009). Using WARP as a marker for inner ear microvasculature, as well, will allow for the anatomical description of human and mice inner ear vasculature and can contribute to our understanding of the inner ear vasculature in normal and pathological entities. The distinct localization of WARP in the human and mouse inner ear blood vessels suggests an important role maintaining the integrity of the vasculature.

4. Experimental Procedures

4.1 Human Specimens

The Institutional Review Board (IRB) of UCLA has approved this study. Appropriate informed consent for inclusion in the study was obtained from each temporal bone donor. The temporal bone donors in the present study are part of a National Institute of Health funded Human Temporal Bone Consortium for Research Resource Enhancement through the National Institute on Deafness and Other Communication Disorders. Temporal bones were obtained at autopsy from five subjects with a documented history of normal auditory and vestibular function. Age ranged from 55-87 years old (four females and one male). The postmortem time ranged from 3 to 12 hours. The vestibular endorgans and cochlea were microdissected from one temporal bone from each donor.

4.2 Human tissue processing

Human Temporal bone removal and vestibular endorgans and cochlea microdissection—At autopsy, the whole brain, including the brainstem and blood vessels, was removed from the cranial cavity. The temporal bones were removed as described by Schuknecht (1968) using a bone plug cutter (Lopez et al., 2005). The bones were then immediately immersed for 16 hours in cold 4% paraformaldehyde in 0.11 M sodium phosphate buffer (PBS), pH 7.4. Thereafter, the fixative was removed by washing with PBS (10 minutes × 3). Temporal bones were placed under a dissecting microscope (Nikon SMZ1500), and the bone surrounding the membranous labyrinth was carefully removed as described previously (Lopez et al., 2005).

Tissue processing for immunohistochemistry: The microdissected utricle, saccule, crista and cochlea were immersed in sucrose 30% (in PBS) for 5 days, and then infiltrated in O.C.T. compound (Tissue Tek, Ted Pella, Redding, CA). Before sectioning, the whole vestibular endorgans and cochlea were placed on Teflon embedding molds (Polysciences Inc., Warrington, PA) and properly oriented (under the dissecting microscope) to obtain longitudinal mid-modiolar serial sections of cochlea, cross sections of the maculae utricle or saccule and of the cristae ampullares. Twenty-micron-thick serial sections were obtained using a cryostat (Microm-HN505E). Sections were mounted on Superfrost plus slides (Fisher Scientific, Pittsburgh, PA) and stored at -80°C until their use. The whole the lateral wall was microdissected from the cochlea and processed for immunohistochemistry as previously described for human vestibular endorgans (Lopez et al. 2005b).

4.3 Immunocytochemistry

Immunofluorescence—The immunofluorescence protocol in the human inner ear has been described previously in detail (Ishiyama et al., 2009, 2010; Lopez et al., 2005, 2007).

Cryostat sections were incubated at room temperature for 60 minutes with a blocking solution containing 1% bovine serum albumin (BSA) fraction-V (Sigma, St. Louis, MO) and 0.5% Triton X-100 (Sigma) in PBS. At the end of the incubation, the blocking solution was removed and the primary polyclonal or monoclonal antibody against the specific protein was applied. WARP (VWA1) rabbit polyclonal affinity purified antibodies raised against von Willebrand factor A domain containing 1 recombinant epitope signature tag, (1:100, cat # HPA035383, Sigma), with an immunogen sequence: PRGDLMFLLDSSASVSHYEFSRVREFVGQLVAPLPLGTGALRASLVHVGSRPYTEFP FGQHSSGEAAQDAVRA were used. Smooth muscle actin (SMA) monoclonal antibodies were used for simultaneous staining and colocalization (1:1000, Sigma St. Louis, Missouri). Primary antibodies were incubated 16 hrs at 4°C. The secondary antibodies against rabbit or mouse labeled with Alexa 488 or 594 (1:1000, Molecular Probes, Carlsbad, CA) were applied and incubated for one hour at room temperature. At the end of the incubation, sections were washed with PBS (3 × 10 minutes) and covered with Vectashield mounting media containing DAPI (Vector Labs, Burlingame, CA).

Paraffin embedding: The microdissected cochlea, vestibular endorgans underwent dehydration by serial immersion for 5 minutes each in increasing concentrations of ethanol: 35%, 50%, 70%, 95% then 100%. The specimens were then transferred to a 1:1 mixture of 100% ethanol and xylene for 5 minutes. Next, the specimens were transferred to a 1:1 mixture of xylene and paraffin and placed in the oven at 65°C for 5 minutes. Tissues were then transferred to paraffin (Paraplast Plus, Polysciences) and placed in the oven for 5 minutes at 65°C. Specimens were properly oriented to obtain mid-modiolar sections of cochlea, cross sections of the cristae ampullaris, maculae utricle and saccule. Twelve-micron-thick paraffin sections were obtained using a microtome. The sections were then immediately mounted in serial fashion on Superfrost plus slides (Fisher Scientific, Pittsburgh, PA). Slides with paraffin-embedded sections were prepared for immunocytochemistry by first undergoing deparaffinization and rehydratation with double distilled water and then PBS.

Indirect immunocytochemistry—For indirect immunocytochemistry, endogenous peroxidase quenching was performed by incubation for 10 minutes with 3% hydrogen peroxide (diluted in 100% in methanol). Slides were then washed with PBS for 10 minutes. Slides were then transferred to a slide carrier filled with antigen retrieval solution (Vector antigen unmasking solution, Vector Labs, Burlingame CA) and heated in the microwave for a total of 5 minutes. The slides were cooled and transferred to a PBS wash for 10 minutes. Sections are incubated for 30 minutes with blocking solution containing 5% normal goat serum(Vector Labs, Burlingame, CA) and 0.5% Triton X-100 (Sigma) in PBS. Incubation with WARP antibody was performed for 48 hours at 4°C in a humid chamber. The sections were washed with PBS (3 × 5 minutes), and then incubated for one hour with biotinylated secondary antibody, goat anti-rabbit polyclonal IgG (1:1000, Vector Labs,). Afterwards, sections were washed PBS (3 × 5 minutes). Next, one hour incubation was performed with Vectastain Elite ABC reagent (Vector Labs) followed PBS wash (5 minutes × 2). Immunoperoxidase staining was performed using Immpact DAB solution (Vector Labs). The reaction was stopped with PBS washes (5 minutes × 3) after 10-15 seconds. Slides were mounted with Vectamount AQ aqueous mounting media and glass cover slips (Vector Labs).

4.2 Mice tissue processing and immunocytochemistry

Mice were handled and cared for in accordance with the Animal Welfare Act and in strict compliance with the National Institute of Health Guidelines. Mice CBA/J mice (6 weeks of age) (N=8, male 8 weeks old,) were over anesthetized with halothane and then decapitated.

Methods for mice tissue processing have been described in detail (Lopez et al., 2005b; Lopez et al., 2009). Fourteen-micron thick cryostat sections were obtained (Microm HM505E) from the mice temporal bones.

Immunohistochemical staining of the mice inner ear—Immunofluorescence and indirect immunohistochemistry using HR-DAB were performed as described below in accordance with Lopez et al., (2005,2009,2010).

Immunohistochemical controls

Positive controls: Cryostat sections from the human and mouse brain and cerebellum were incubated with the antibodies against WARP. The immunolocalization was similar to previous reports in the cerebral vasculature (Allen et al., 2008). Cochlear tissue sections from mice cochlea were incubated without the primary antibodies. Figure 6 shows results from the positive and negative controls. Western blot was performed to determine the quality of the WARP antibody (Fig. 7, see description below).

Microscopic observation and documentation—The human and mice inner ear and immunocytochemical control sections were viewed and imaged with an Olympus BX51 fluorescent microscope (Olympus America Inc, NY, USA) equipped with an Olympus DP70 digital camera. To provide unbiased comparisons of the immunoreactive signal between each specimen, all images were captured using strictly the same camera settings. Images were acquired using MicroSuite™ Five software (Olympus America Inc). Images were processed using the Adobe Photoshop™ software program run on a Macintosh iMAC computer. Confocal images were acquired using a Carl Zeiss Laser Scanning Microscope 5 Exciter Vario2, RGB V4.2 (Jena, Germany).

4.3 Western blot using the WARP antibody

Ten whole mice inner ear from 5 mice (microdissected whole cochlea and vestibule), and human cerebellum (small portion of the cortex, 0.5g) were individually immersed in 1:20 (W/V) of tissue T-PER (tissue protein extraction reagent, Pierce, Rockford, IL) with protease inhibitor cocktail (Roche, Basel, Switzerland), and mechanically disrupted by sonication. The samples were centrifuged for 2 minutes at 12000 rpm. The supernatant was collected for protein quantification (Quanti-iT protein assay quit, Invitrogen) and separation. Reduced samples were prepared; in LDS sample buffer (NuPAGE, Invitrogen), reducing agent (NuPAGE, Invitrogen) and deionized water (1:1). Samples were heated at 75°C for 10 minutes and samples proteins were separated in 10% polyacrylamide-SDS gels (NuPAGE 10% Bis-Tris mini gel, Invitrogen). Proteins were transferred to polyvinylidene fluoride (PVDF) membranes (Invitrogen, USA) and detected with a 1:1000 dilution of WARP antibody (dilution buffer). β-actin monoclonal antibody (1:2000; Sigma SLM) was used as control. Bound antibodies were visualized using WesternBreeze chromogenic immunodetection kit (Invitrogen, Carlsbad CA, USA). The WARP rabbit polyclonal antibody produced a band of approximately 50-60 KDa in the mouse inner ear and in the human cerebellum, and two additional bands of 60-80 kDa in the human cerebellum (Figure 7A). A band of 40-50 kDa corresponding to b-actin in the mice cochlea is shown as positive control (Fig 7B)

Acknowledgments

National Institutes of Health Grants, National Institute on Deafness and Other Communication Disorders DC 005028 and 5U24 DC 008635. We acknowledge Dr Dwayne Simmons and Mr. Arian Nasiri from the Life Sciences Department at UCLA for the acquisition of the laser confocal microscope images.

Abbreviations

WARP	von Willebrand A domain-related protein
VWA1	Von Willebrand factor A domain containing 1
VWF	Von Willebrand factor
SMA	smooth muscle actin

References

Allen JM, Bateman JF, Hansen U, Wilson R, Bruckner P, Owens RT, Sasaki T, Timpl R, Fitzgerald J. WARP is a novel multimeric component of the chondrocyte pericellular matrix that interacts with perlecan. J Biol Chem. 2006; 281:7341–7349. [PubMed: 16407285]

Allen JM, Brachvogel B, Farlie PG, Fitzgerald J, Bateman JF. The extracellular matrix protein WARP is a novel component of a distinct subset of basement membrane. Matrix Biol. 2008; 27:295–305. [PubMed: 18314316]

Allen JM, Zamurs L, Brachvogel B, Schlotzer-Schrehardt U, Hansen U, Lamande SR, Rowley L, Fitzgerald J, Bateman JF. Mice Lacking the Extracellular Matrix Protein WARP Develop Normally but Have Compromised Peripheral Nerve Structure and Function. J Biol Chem. 2009; 284:12020–12030. [PubMed: 19279005]

Axelsson A. The vascular anatomy of the cochlea in the guinea pig and in man. Acta Otolaryngol. 1968; 234(Suppl):1–243.

Bachor E, Selig YK, Jahnke K, Rettinger G, Karmody CS. Vascular variations of the inner ear. Acta Otolaryngol. 2001; 121:35–41. [PubMed: 11270491]

Bhattacharya G, Miller C, Kimberling WJ, Jablonski MM, Cosgrove D. Localization and expression of usherin a novel basement membrane protein defective in people with Usher's syndrome type IIa. Hear Res. 2002; 163:1–11. [PubMed: 11788194]

Colombatti A, Bonaldo P. The superfamily of proteins with von Willebrand factor type A-like domains: one theme common to components of extracellular matrix, hemostasis, cellular adhesion, and defense mechanisms. Blood. 1991; 77:2305–15. [PubMed: 2039815]

Cosgrove D, Samuelson G, Pinnt J. Immunohistochemical localization of basement membrane collagens and associated proteins in the murine cochlea. Hear Res. 1996; 97:54–65. [PubMed: 8844186]

Cosgrove D, Samuelson G, Meehan DT, Miller C, McGee J, Walsh EJ, Siegal M. Ultrastructural, physiological and molecular defects in the inner ear of gene-knockout mouse model for autosomal Alport syndrome. Hear Res. 1998; 121:84–98. [PubMed: 9682811]

Dityatev A, Frischknect R, Seiderbecher CI. Extracellular matrix and synaptic functions. Results Probl Cell Differ. 2006; 43:69–97. [PubMed: 17068968]

Duball AJ, Santi PA, Hukee MJ. Cochlear fluid balance: A clinical/research overview. Ann Otol Rhinol Laryngol. 1980; 89:335–41. [PubMed: 6774652]

Eble JA, Noland S. The extracellular matrix of blood vessels. Curr Pharm Dis. 2009; 15:1385–400.

Fitzgerald J, Ting ST, Bateman JF. WARP is a new member of the von Willebrand factor A-domain superfamily of extracellular matrix proteins. FEBS Letters. 2002; 517:61–66. [PubMed: 12062410]

Hawkins JE Jr. Comparative otopathology: Aging, noise and ototoxic drugs. Adv Otorhinolaryngol. 1973; 20:125–141. [PubMed: 4710505]

Hawkins JE Jr. Microcirculation in the labyrinth. Arch Otorhinolaryngol. 1976; 212:241–51. [PubMed: 990077]

Heinegard D. Proteoglycans and more- from molecules to biology. Int J Exp Path. 2009; 90:575–586. [PubMed: 19958398]

Ishiyama A, Mowry SE, López IA, Ishiyama G. Immunohistochemical distribution of basement membrane proteins in the human inner ear. Hearing Res. 2009; 254:1–14.

Ishiyama G, Tokita J, Lopez I, Tang Y, Ishiyama A. Unbiased stereological estimation of the spiral ligament and stria vascularis volumes in aging and Meniere's disease using archival human temporal bones. JARO. 2007; 8:8–17. [PubMed: 17160359]

Ishiyama G, Lopez IA, Beltran-Parrazal L, Ishiyama A. Immunohistochemical localization and mRNA expression of aquaporins in the macula utricle of patients with Meniere's disease and acoustic neuroma. Cell Tissue Res. 2010; 340:407–19. [PubMed: 20461409]

Lawrence M. Control mechanisms of inner ear microcirculation. Am J Otolaryngol. 1980; 1:324–33. [PubMed: 7004224]

Learly SE, Mescher JM, Sewel WF, Tao SL, Borenstein JT. Inner ear drug delivery for auditory applications. Adv Drug Delivey Reviews. 2008; 60:1583–99.

Lopez I, Ishiyama G, Tang Y, Frank M, Baloh RW, Ishiyama A. Estimation of the number of nerve fiber in the human vestibular endorgans using unbiased stereology and immunohistochemistry. Journal Neurosci Methods. 2005; 145:37–46.

Lopez I, Acuna D, Galbraith G, Bok D, Ishiyama A, Liu W, Kurtz I. Time course of auditory impairment in mice lacking the electroneutral sodium bicarbonate cotransporter NBC3 (slc4a7). Dev Brain Res. 2005b; 160:63–77. [PubMed: 16181686]

Lopez IA, Ishiyama G, Lee M, Baloh RW, Ishiyama A. Immunohistochemical localization of aquaporins in the human inner ear. Cell & Tissue Res. 2007; 328:453–460. [PubMed: 17318586]

Lopez IA, Rosenblatt MI, Kim C, Galbraith GG, Jones SM, Kao L, Newman D, Liu W, Yeh S, Pushkin A, Abuladze A, Kurtz I. Slc4a11 gene disruption in mice: Cellular targets of sensorineuronal abnormalities. J Biol Chem. 2009; 284:26882–96. [PubMed: 19586905]

Lopez IA, Acuna D, Shahram Y, Mowlds D, Ngan AM, Rungvivatjarus, Sharma Y, Edmond J. Neuroglobin expression in the cochlea of rat pups exposed to chronic very mild carbon monoxide (25 ppm) in air during and after the prenatal period. Brain Res. 2010; 1327:56–68. [PubMed: 20211612]

McCall A, Ishiyama G, López IA, Sunita B, Ishiyama A. Histopathological and ultrastructural analysis of vestibular endorgans obtained from patients with Meniere's disease. BMC Ear Nose Throat Disord. 2009; 3;9:4.

Masutani H, Takashi H, Sando I. Stria vascularis in Meniere's disease: A quantitative histopathological study. Auris Nasus Larynx. 1992; 19:145–52. [PubMed: 1489279]

Mazzoni A. The vascular anatomy of the vestibular labyrinth in man. Acta oto-laryngologica (Suppl). 1990; 472:1–83.

Miller JM, Ren TY, Nuttall AL. Studies of inner ear blood flow in animals and humans. Otolaryngol Head Neck Surg. 1995; 112:101–113. [PubMed: 7816443]

Nakashima T, Naganawa S, Sone M, Tominaga M, Hayashi H, Yamamoto H, Liu X, Nuttall AL. Disorders of cochlear blood flow. Brain Res Brain Res Rev. 2003; 43:17–28. [PubMed: 14499459]

Rehm HL, Zhang DS, Brown MC, Burgess B, Halpin C, Berger W, Morton CC, Corey DP, Chen ZY. Vascular defects and sensorineural deafness in a mouse model of Norrie disease. J Neurosci. 2002; 22:4386–4292.

Rodriguez CI, Cheng JG, Liu L, Stewart CL. Cochlin, a secreted von Willebrand factor type A domain-containing factor, is regulated by leukemia inhibitory factor in the uterus at the time of embryo implantation. Endocrinology. 2004; 145:1410–1418. [PubMed: 14657014]

Robertson NG, Cremers CW, Huygen PL, Ikezono B, Krastins B, Kremer H, Kuo SF, Liberman MC, Merchant SN, Miller CE, Nadol JB, Sarracino DA, Verhagen WI, Morton CC. Cochlin immunostaining of inner ear pathologic deposits and proteomic analysis in DFNA9 deafness and vestibular dysfunction. Hum Mol Genet. 2006; 15:1071–1085. [PubMed: 16481359]

Rodgers KD, Barrit L, Miner JH, Cosgrove D. The laminins in the murine inner ear: developmental transitions and expression in cochlear basement membranes. Hear Res. 2001; 158:39–50. [PubMed: 11506935]

Shi X, Han W, Yamamoto H, Tang W, Lin X, Xiu R, Trune DR, Nuttal AI. The cochlea pericytes. Microcirculation. 2008; 15:515–529. [PubMed: 19086261]

Shi X. Cochlear pericyte responses to acoustic trauma and the involvement of hypoxia-inducible factor-1α and vascular endothelial growth factor. Am J Pathology. 2009; 174:1692–1704.

Smith CA. Structure of the stria vascularis and spiral prominence. Ann Otol Rhinol Laryngol. 1957; 66:521–36. [PubMed: 13459248]

Takahashi M, Hokunan K. Localization of type IV collagen and laminin in the guinea pig inner ear. Ann Otol Rhinol LAryngol. 1992; 101:58–62.

Tsuprun T, Santi P. Proteoglycan arrays in the cochlear basement membrane. Hear Res. 157:65–76. [PubMed: 11470186]

Warchol ME, Speck JD. Expression of GATA3 and tenascin in the avian vestibular maculae: normative patterns and changes during sensory regeneration. J Comp Neurol. 2007; 500:646–657. [PubMed: 17154269]

Wehrle B, Chiquet M. Tenascin is accumulated along developing peripheral nerves and allows neurite outgrowth in vitro. Development. 1990; 110:401–415. [PubMed: 1723942]

Whittaker CA, Hynes RO. Distribution and evolution of von Willebrand integrin A domains: widely dispersed domains with roles in cell adhesion and elsewhere. Mol Biol Cell. 2002; 13(10):3369–3387. [PubMed: 12388743]

Xu Q, Wang Y, Dabdoub A, Smallwood PM, Williams J, Woods C, Kelley MW, Jiang L, Tasman W, Zhang K, Nathans J. Vascular development in the retina and inner ear: control by Norrin and Frizzled-4, a high-affinity legend-receptor pair. Cell. 2004; 116:883–895. [PubMed: 15035989]

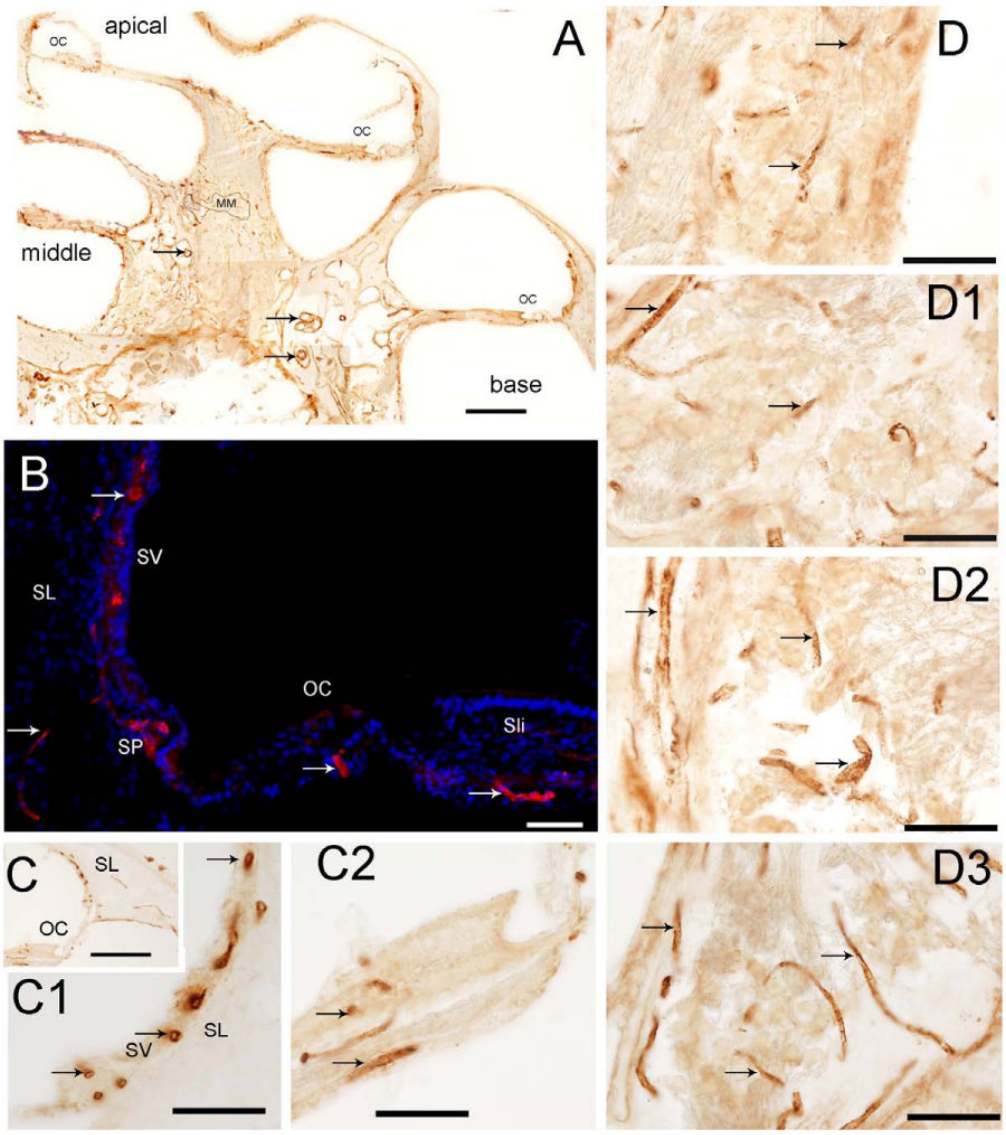

Fig 1.

WARP immunoreactivity (-IR) distribution in the human cochlea. (A) Low magnification view of WARP-IR (visualized with diaminobenzidine DAB, amber color) in the human cochlea. Arrows point to blood vessels stained with WARP. (B) WARP-IR visualized with secondary antibodies labeled with Alexa 596, (red color), dapi in blue color identified cell nuclei. WARP-IR was present in blood vessels of the spiral ligament (SL), the stria vascularis (STV) and basilar membrane underneath the organ of Corti (OC), Spiral limbus (SLi). Arrows point to blood vessels stained with WARP. (C) WARP-IR in the hook region of the cochlea. (C1) High magnification view shows WARP-IR in blood vessel of the SV. (C2) High magnification view shows WARP-IR in blood vessels of the Sli. Panels D, D1, D2 and D3 show WARP-IR in blood vessels of the spiral ganglia of the apical, middle, basal and hook region of the cochlea. Bar is A) 500 μm, B) 50 μm, C) 250 μm, C1) and C2) 30 μm. D-D3) 100 μm.

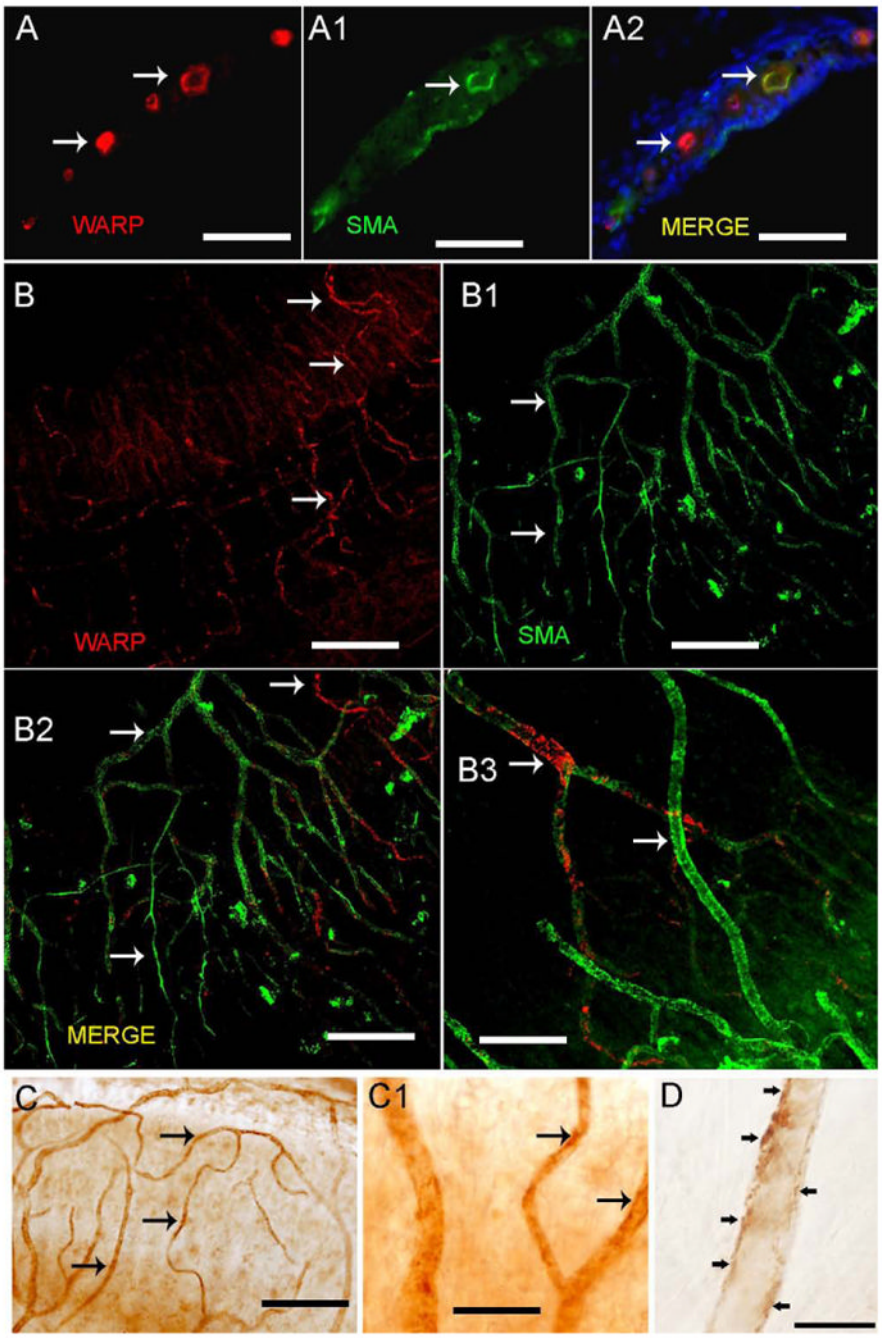

Fig 2.

WARP-IR and SMA-IR in the stria vascularis and lateral wall of the human cochlea. (A) WARP-IR (red color) in blood vessels of the stria vascularis, Figure A1 shows the same section stained with antibodies against SMA (green color). Figure A2 is a merge image from A and A1. Arrows point to blood vessels stained with WARP and SMA-IR. Fig B shows a surface preparation of the lateral wall of the cochlea (middle to basal portion). WARP-IR (in red color) is present in blood vessels of the lateral wall. Figure B1 shows the same preparation stained with antibodies against SMA (green color). Figure B2 is a merged image from B and B1. (B3) is a high magnification view (B-B3 are representative optical sections produced by laser confocal microscopy). (Fig C) Immunoreactivity of WARP with DAB

shows the immunostaining of the dense network of blood vessels. Fig C1 shows a high magnification view from Fig C which shows that the internal portion of the blood vessels is WARP-IR. Fig D shows a thin section of the spiral ligament. Arrows point to WARP-IR in blood vessels. Magnification bar in A, A1 and A2) 50 μm, B, B1 and B2) 500 μm, B3) 200 μm. C) 125 μm, C1) 50 μm, D) 20 μm.

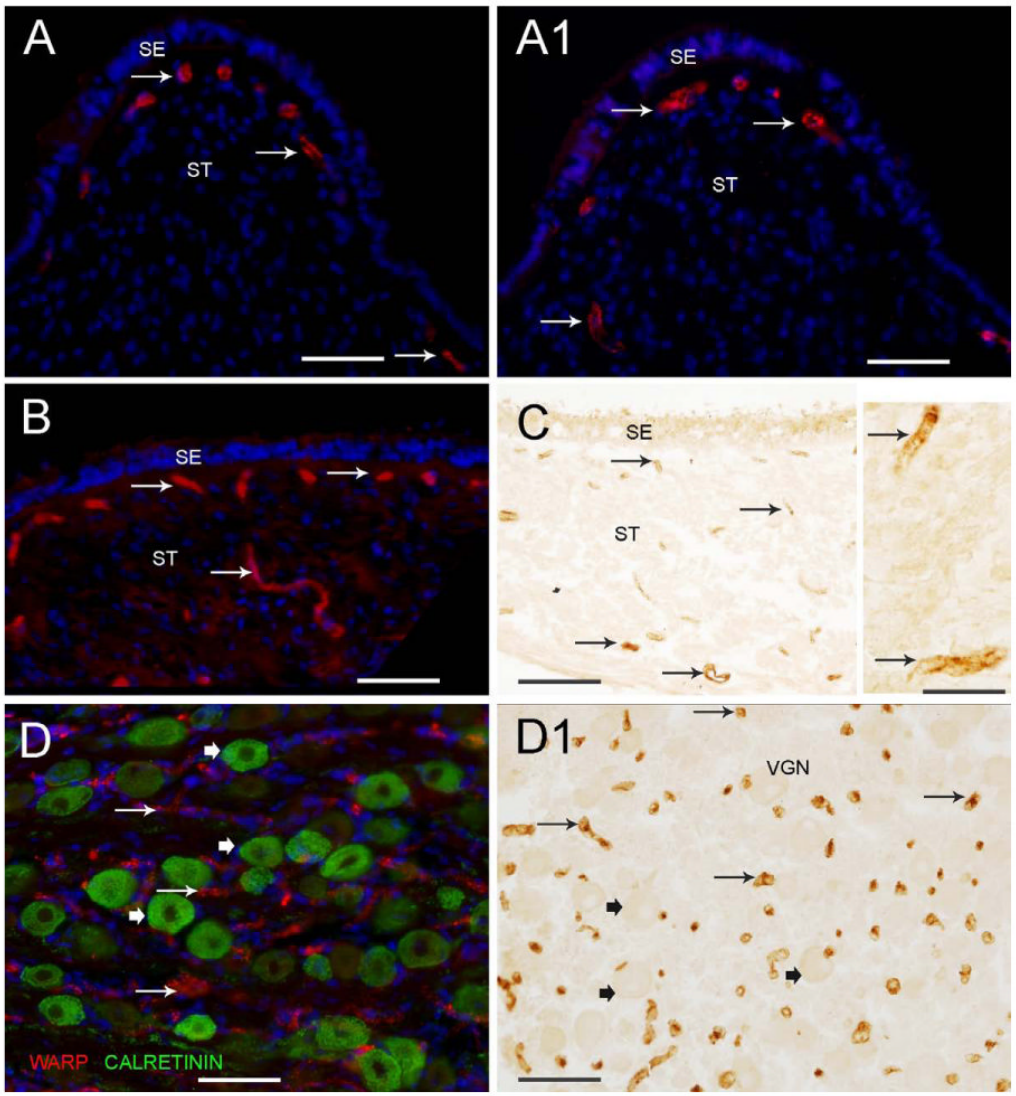

Fig 3.

WARP-IR in the human vestibular endorgans. Figure A and A1 show WARP-IR, in the central and peripheral portion of the horizontal crista ampullaris. WARP-IR (red color) was localized in blood vessels running throughout the stroma (arrows). The sensory epithelia (SE) showed no immunoreactivity. (B) The maculae utricle demonstrated WARP-IR in the vasculature within the stroma. (C) Immunoreactivity of WARP with DAB in a cross section of maculae sacule demonstrated WARP-IR in the vasculature within the stroma. (D) WARP-IR (red color) and calretinin (green color) in the vestibular ganglia. Calretinin positive neurons were not immunoreactive for WARP. (D). Immunoreactivity of WARP with DAB, WARP was confined to blood vessels. Spiral ganglia neurons (SGN) were not reactive for WARP. Magnification bar in A, A1, B and C) 100 μm, A1, B1, C and C1) 25 μm, and D) 100μm.

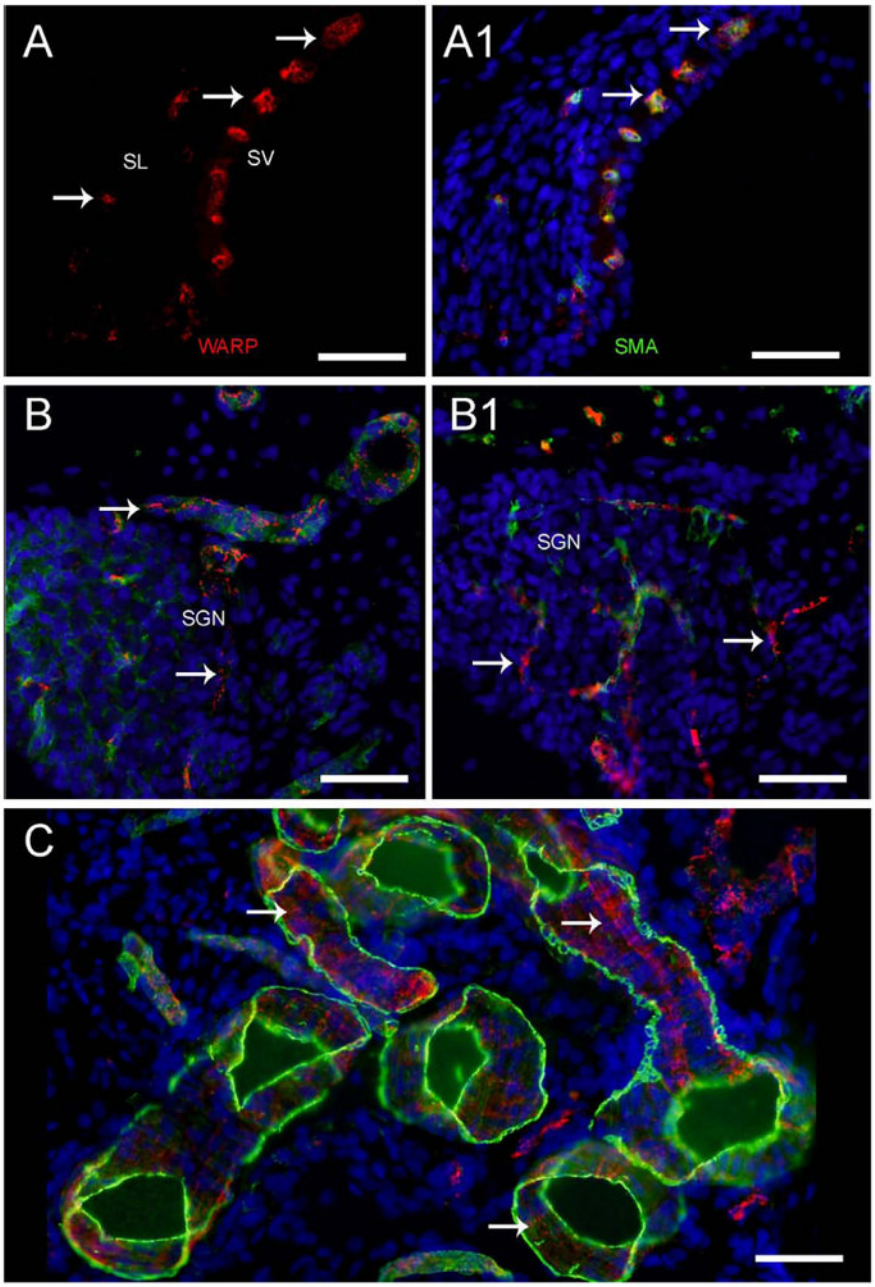

Fig 4.

WARP-IR in the mouse cochlea. (A) WARP-IR (arrows) was present in the vasculature of the spiral ligament, and the stria vascularis. Fig (A1) shows colocalization WARP-IR and SMA (green color) in the stria vascularis blood vessels (same section from (A). Figure B and B1 shows WARP-IR and SMA in blood vessels of the spiral ganglia (middle and basal portion). Spiral ganglia neurons (SGN) were not immunoreactive. (C) Colocalization of WARP and SMA in blood vessels of the mid-modiolus of the mice cochlea. Magnification bar in A, and A1) 30 μm, B and B1) 100 μm, C) 20 μm.

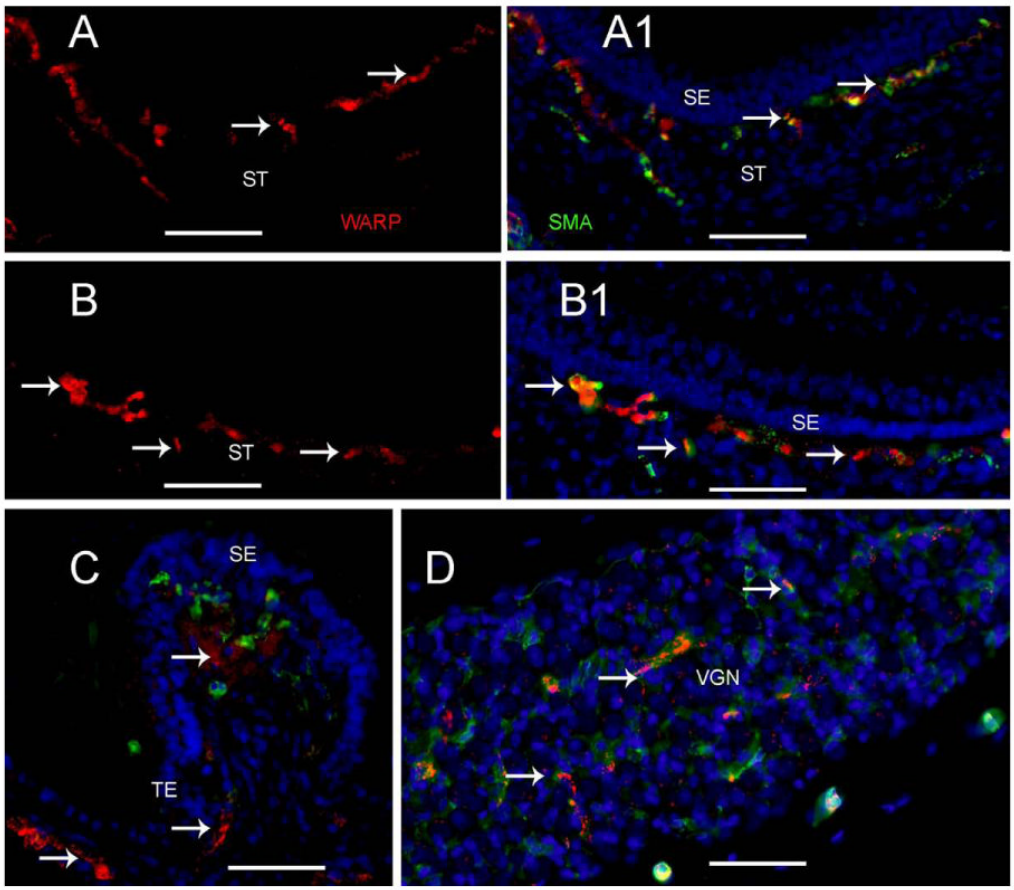

Fig 5.

WARP-IR in the mouse vestibular endorgans. Figure A shows WARP-IR (immunofluorescence) in the macula utricle. WARP-IR was seen in stromal blood vessels (arrows). (A1) WARP and SMA colocalization (same section from A) in stromal blood vessels. The sensory epithelia show no WARP-IR. (B) The maculae saccule revealed a similar distribution of WARP-IR in stromal blood vessels. (B1) WARP and SMA colocalization (same section from B) in stromal blood vessels. (C) The horizontal crista ampullaris showing WARP and SMA colocalization (same section from B) in stromal blood vessels. (D) WARP and SMA colocalization in blood vessels of the vestibular ganglia. Magnification bar in A, A1, B, B1 and C) 50 μm, D) 150 μm.

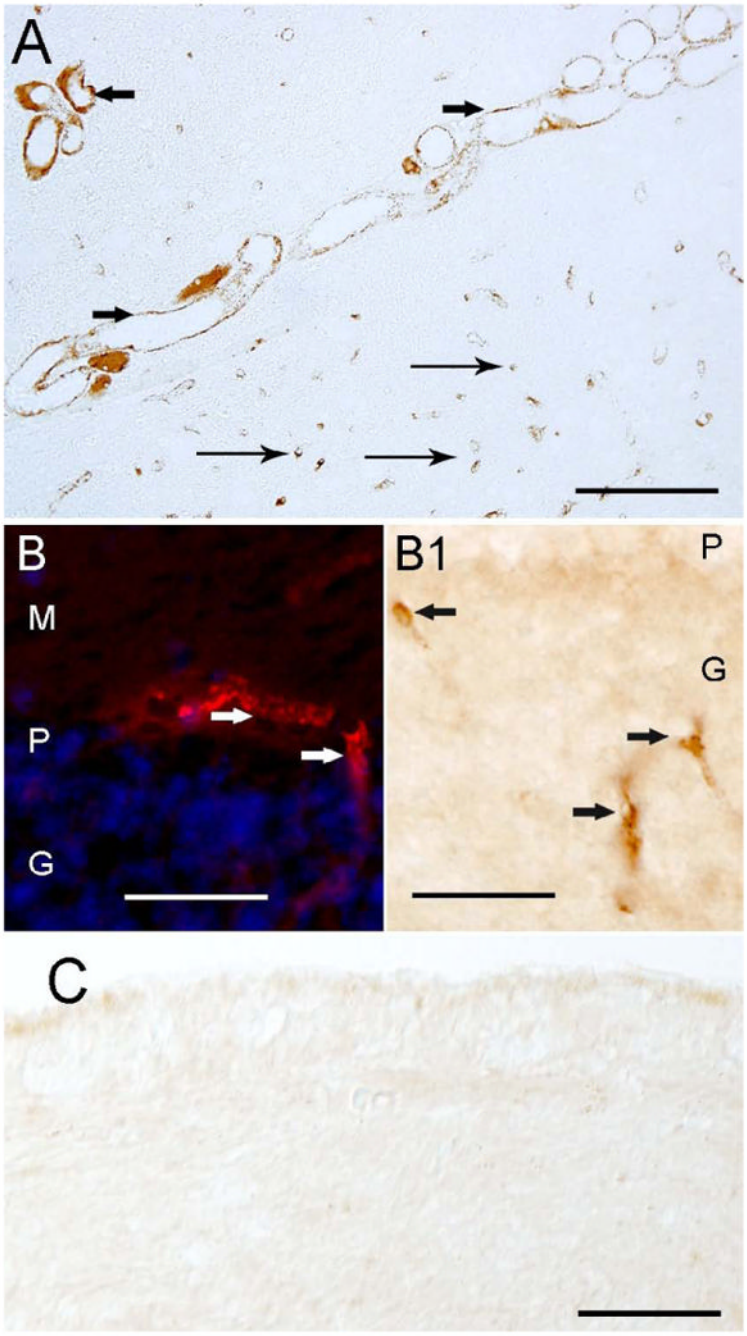

Fig 6.

WARP-IR controls. (A) Shows WARP-IR in thick (arrowheads) and thin (arrows) blood vessels (luminal portion) of the human brainstem (Pons). (5B and 5B1) shows WARP-IR in blood vessels (arrowheads) of the mouse cerebellar cortex. (M: molecular, P: Purkinje, G: granular layers). (4C) shows a cross-section of the human utricle immunostained with all the reagents except for the WARP antibody and no specific reaction was observed. Magnification bar in A= 250 μm, B and B1= 100 μm, C= 30 μm.

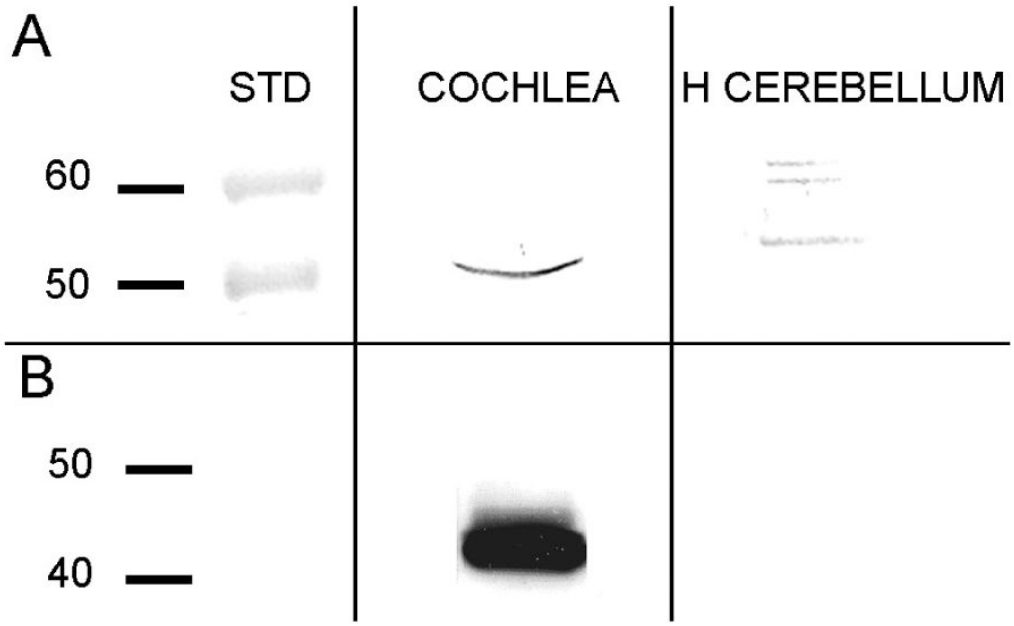

Fig 7.
(A) Western blot of the mice cochlea and human cerebella extracts probed with the rabbit anti-WARP polyclonal antibody or (B) b-actin monoclonal antibody. Migration positions of molecular weight markers (kDa) are indicated on the left.